Basic Relations for Control of Flexible Vehicles

WILLIAM B. GEVARTER*
Bellcomm Inc., Washington, D. C.

Papers written on the control of flexible vehicles have primarily concerned themselves with a particular example or a particular class of vehicles. Even in these restricted studies, computer solutions are generally used and little insight is offered into the basic initial approach to designing a "control system/flexible vehicle" combination from scratch. Therefore, in this paper an attempt is made to indicate the basic relationships that enter into the control of flexible vehicles, and to show that these relationships are the same for a variety of flexible vehicle types and are not limited to those displaying only bending modes. Further, for several fundamental cases, simple analytic approximations are presented for the system characteristic roots, which can both guide the system design and provide a measure of the system response. The approach is illustrated by comparing the analytic approximations with computer results for several simple vehicles.

Nomenclature

a_n = μ_n/q_n, the factor converting the nth mode generalized coordinate to the quantity sensed by the feedback instrument
$f(x)$ = force per unit length
g = acceleration of gravity
j = square root of -1
k = K_p/p_i^2
k' = K_v/p_i
$m(x)$ = mass per unit length
p_n = nth mode natural frequency
q_n = nth mode generalized coordinate
r_n = p_n/p_i
$\bar{r}$ = radius vector from the vehicle center of mass
$\Delta\bar{r}$ = vector deflection
s = Laplace operator
$\bar{s}$ = s/p_i
$\bar{s}_i$ = $s_i/p_i = \epsilon + j(1 + \delta)$, normalized system characteristic root (in the upper half plane) associated with the ith mode
t = time
u_n = Q_n/Q_c, the factor converting the rigid mode control Q_c to the nth mode generalized forcing function, $Q_n.u_n$ is positive if the + directions of the force and $w_n(x_f)$ are the same.
$\bar{w}_n(\bar{r})$ = normal mode of free vibration
x = distance along longitudinal axis from end of vehicle
F = force
F_n = nth mode generalized force; defined by Eq. (4)
$G(s)$ = transfer function of equivalent plant; defined by Eq. (9)
I = mass moment of inertia about the pitch axis
K_p = position gain
K_v = velocity gain
L = length of vehicle
M = mass of vehicle
M_n = nth mode generalized mass; defined by Eq. (3)
Q_c = rigid mode forcing function
Q_n = F_n/M_n, nth mode forcing function
R = $L/2$
T_n = the Laplace transfer function of the nth mode; defined by Eq. (6)
δ = imaginary portion of the departure of $\bar{s}_i$ from the normalized ith mode pole
ϵ = real portion of $\bar{s}_i$
ζ_n = nth mode equivalent viscous damping
μ = a rigid body motion we desire to control (such as a rotation or translation)
ξ = x/L

Subscripts

c = control
co = rigid mode parameter with control
f = force
n,m,i = integers; nth, mth, and ith modes of vibration
o = rigid mode parameter without control
s = sensed
ref = reference control input

Presented as Paper 69-115 at the AIAA 7th Aerospace Sciences Meeting, New York, January 20–22, 1969; submitted January 27, 1969; revision received August 13, 1969. This paper is based in part on a Stanford University Ph.D. dissertation[3] under R. H. Cannon Jr.

* Member of the Technical Staff; presently on the staff of the Office of Policy, NASA, Washington, D.C. Member AIAA.

I. Introduction

THIS paper is intended to provide an orderly introduction to the subject of elastic vehicle and control system interaction. As such, it presents a simple model of the system, the associated equations, simple approximations to the system characteristic roots, physical interpretations of the associated phenomena, and some basic design considerations. The ideas presented are illustrated by application to several simple vehicles.

From the point of view of stability, if a vehicle were rigid the locations of the control sensors and actuators (control forces or moments) would be unimportant. However, when flexure is considered, these locations are of the utmost importance because they determine the coupling of the flexural motions to the rigid body motion to be controlled. This coupling can lead to instability, an effect which has often been observed.

Unfortunately, the fundamental relationships between sensor and actuator locations and the flexural modal response in a vehicle with automatic control (needed to properly initiate a design or to make needed modifications) have been in general masked by the complexity of the problem. References 1 and 2 partially recognized these relationships, but no closed form analytical solutions were offered, so that the effect on stability could not be clearly discerned. Therefore, this paper is devoted to these relationships, with approximate closed form analytic solutions being developed to determine the system's characteristic roots, furnish stability criteria, and to provide an indication of the real time response.

II. A Cybernetic Model of a Flexible Vehicle

The basic form of the equations of motion of uncontrolled flexible vehicles of arbitrary shape are presented in detail in Ref. 3 and summarized below. We will first indicate why the natural vibrations of a vehicle are uncoupled from the rigid body motions and then show the manner in which coupling between these motions occurs due to control.

Using these results, a cybernetic model is obtained indicating the informational flow coupling the flexural modes to the rigid body mode we desire to control. In this paper we will limit ourselves to the common problem of flexible vehicles with control systems having uncoupled control axes (coupled neither through the rigid body control nor thru flexure). The reader is referred to Ref. 3 for the treatment of vehicles having coupled axes.

Because they impose no external forces, natural vibrations of a vehicle do not change the linear momentum or the angular momentum of the system. Thus we find that, for a flexible vehicle, we can usually express the equations of rigid body motion as being uncoupled from the equations of vibration.†

The vehicle vector deflection $\Delta\bar{r}$, at a location $\bar{r}$ from the vehicle center of mass, can be approximately expressed in terms of the first N normal modes of free vibration, $\bar{w}_n(\bar{r})$, as

$$\Delta\bar{r}(\bar{r},t) = \sum_{n=1}^{N} q_n(t)\bar{w}_n(\bar{r}) \tag{1}$$

When this is done for nonspinning vehicles (or for spinning vehicles whose deflection is in the direction of the spin vector or is purely torsional deflection about the spin axis), the equations of vibration (making use of the orthogonality conditions of the normal modes) appear in linearized form as‡

$$\ddot{q}_n + 2\zeta_n p_n \dot{q}_n + p_n^2 q_n = F_n/M_n \triangleq Q_n \tag{2}$$

where

$$M_n \triangleq \int_V \rho\bar{w}_n(\bar{r})\cdot\bar{w}_n(\bar{r})\,dV = [n\text{th mode generalized mass}] \tag{3}$$

$$F_n \triangleq \int_V \frac{\partial\bar{F}}{\partial V}\cdot\bar{w}_n(\bar{r})\,dV = [n\text{th mode generalized force}] \tag{4}$$

q_n = nth mode generalized coordinate, p_n = nth mode natural frequency, ζ_n = nth mode equivalent viscous damping approximation to the structural damping, $\rho(\bar{r})$ = mass density, $d\bar{F}$ = force acting on a mass particle, V = volume.

Neglecting disturbances, the equation of motion of a rigid body motion μ, that we desire to control, usually appears as

$$\ddot{\mu} + 2\zeta_o p_o \dot{\mu} + p_o^2 \mu = Q_c \tag{5}$$

where p_o = rigid mode natural frequency, usually equal to zero, ζ_o = rigid mode damping ratio without control, Q_c = rigid body control function.

Observe that the equations for the flexible motions, Eq. (2), and the rigid body motion, Eq. (5), appear in uncoupled form except for coupling that might occur through the forcing functions. When a feedback control system is applied, this coupling can take place as follows:

1) The sensors designed to sense the rigid motion sense the flexible motion as well.

2) The forces and moments applied to control the rigid body motion also excite the flexible motions.

This interaction of the rigid and flexible motions and the control system is shown in the cybernetic model given in Fig. 1, where

$$T_n \triangleq 1/(s^2 + 2\zeta_n p_n s + p_n^2) \tag{6}$$

the Laplace transfer function of the nth mode. This figure is

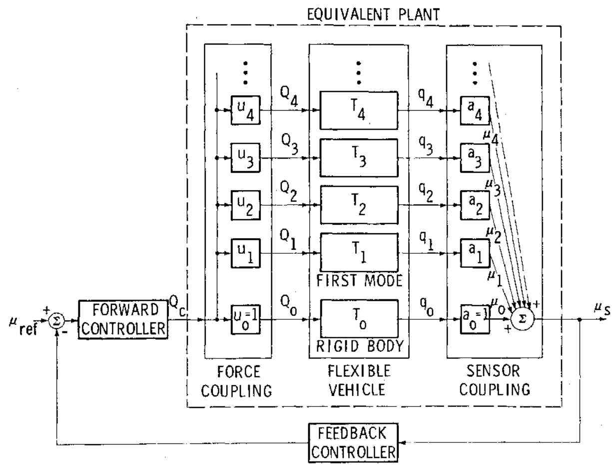

Fig. 1 Cybernetic model of one axis of a flexible vehicle employing a feedback control system having uncoupled control axes.

applicable for both linear and nonlinear feedback control systems.

In Fig. 1, u_n represents the factor converting the rigid-body control, Q_c, to the nth mode generalized forcing function, Q_n

$$u_n = Q_n/Q_c \tag{7}$$

and a_n represents the factor converting the nth mode generalized coordinate to the quantity sensed by the feedback sensor (or sensors)

$$a_n = \mu_n/q_n \tag{8}$$

The factors u_n and a_n are determined in sign and magnitude by the location of the control force and sensor, respectively, with respect to the nth mode shape. For small deflections, linear sensors, and the actuators (control forces and moments) and sensors at fixed locations, the u_n's and a_n's can usually be taken as constants.

Considering the first N flexural modes, for purposes of control the transfer function for the equivalent plant can be written directly from Fig. 1 as

$$G(s) = \sum_{n=0}^{N} \frac{u_n a_n}{s^2 + 2\zeta_n p_n s + p_n^2} \tag{9}$$

Observe that for each mode the coupling parameters u_n and a_n (henceforth considered as constants) always occur as a product in the control equations and can be treated as a unit in control problems.

III. Flexible Vehicles Employing Simple Linear Feedback Control

To obtain analytic results, we will apply the cybernetic model just developed to the important class of vehicles which employ linear feedback control. In this paper we will treat in detail only simple position and rate feedback control systems. However extension to any other linear control system is straightforward. In this section we will develop the equations for such systems and discuss the difficulties of obtaining solutions by the conventional root locus method without the aid of a computer.

To control a rigid body motion μ about a reference value, a control function of the following form is commonly chosen

$$Q_c = -K_v(d/dt)\mu - K_p(\mu - \mu_{\text{ref}}) \tag{10}$$

Substituting Eq. (10) into Eq. (5) yields (when flexure is neglected)

$$\ddot{\mu} + 2\zeta_{co}p_{co}\dot{\mu} + p_{co}^2\,\mu = K_p\mu_{\text{ref}} \tag{11}$$

† In certain cases vibration can significantly influence the direction of applied forces and thereby affect rigid body motion. For simplicity, this form of coupling will be neglected in this paper.

‡ A derivation of this equation for lumped parameter systems is given in Ref. 4.

where

$$p_{co} = (p_o^2 + K_p)^{1/2} \tag{12}$$

and for ζ_o negligible compared to the damping furnished by the controller,

$$\zeta_{co} = K_v/2p_{co} \tag{13}$$

(Ref. 5 indicates that desirable values of ζ_{co} are 0.7 to 0.8, so that this range will be used for the numerical examples given later.) For the control law given by Eq. (10), the system transfer function is simply

$$\mu_s(s)/\mu_{ref}(s) = K_pG(s)/[1 + (K_vs + K_p)G(s)] \tag{14}$$

where $G(s)$ is given by Eq. (9).

The characteristic equation is

$$1 + (K_vs + K_p)G(s) = 0 \tag{15}$$

which can also be written as

$$[1 + K_pG(s)]\{1 + K_vsG(s)/[1 + K_pG(s)]\} = 0 \tag{16}$$

The roots of this equation can be found, in principle, by using a double root locus plot: first plotting the locus of roots with respect to K_p and then, for K_p fixed, plotting the locus of roots with respect to K_v.§ However, the zeros of $G(s)$ are not readily available, so that the solution of a quartic is required when two flexible modes are included, the order of the equation rising by two for each additional mode. The effort can be halved if damping is neglected in finding the zeros; but the over-all effort is still considerable if we include the higher modes.

Because of the difficulty involved in determining the system stability and characteristic roots by conventional analytical and graphical methods, we devote the next section to developing simple formulas for determining the stability and estimating the system characteristic roots of flexible vehicles employing linear feedback control systems with uncoupled control axes. These approximate analytic solutions provide greater insight than would be obtained by numerical solutions.

IV. A General Method for Studying Stability and Estimating Real Time Response for Linear Systems with Uncoupled Axes

In this portion a general method is developed for studying the stability, finding the system characteristic roots, and providing an indication of the real time response of flexible vehicles employing linear feedback control, whose control axes can be considered uncoupled. The approach is to expand the characteristic roots about their normalized modal poles.

In Section A we develop a stability criterion and estimate the roots for small gains for the simple rate and position feedback control. This development is extended in Sec. B to include more complex control systems. Sections C and D provide an indication of the real time response of the system and a physical interpretation of the results. The effects of sensor and control locations on system stability for a simple vehicle are illustrated in Sec. E.

A. Stability and Characteristic Roots for Small Effective Gains—Simple Rate and Position Feedback Control Case

A much simpler approach than the conventional root locus method for studying stability is to expand the characteristic roots about the normalized modal poles. Observe that in Eq. (15), if we neglect the small structural damping ratio ζ_n, there are no roots on the imaginary axis, except for $K_v = 0$ and $K_v = \infty$, so that the loci associated with K_v never cross the imaginary axis. Thus, if a root starts off into the left half plane, it will remain stable for all gains, whereas if it starts off into the right half plane, it will always be unstable. Small structural damping displaces the root locus to the left but does not change the relative character of the results. Therefore, to determine if a locus associated with the ith mode is stable, it is necessary only to determine its behavior in the vicinity of the ith mode pole. This is the customary problem of determining departure directions for the loci.

To normalize the ith mode pole, the numerator and denominator of each term of $G(s)$ in Eq. (15) are divided by p_i^2 to obtain

$$1 + (k'\bar{s} + k) \sum_{n=0}^{N} \frac{u_na_n}{\bar{s}^2 + 2\zeta_nr_n\bar{s} + r_n^2} = 0 \tag{17}$$

where

$$\bar{s} \triangleq s/p_i \tag{18}$$

$$r_n \triangleq p_n/p_i \tag{19}$$

$$k' \triangleq K_v/p_i = \text{effective velocity gain for the } i\text{th mode} \tag{20}$$

$$k \triangleq K_p/p_i^2 = \text{effective position gain for the } i\text{th mode} \tag{21}$$

Because of this normalization, for small gains the root near the ith mode pole in the upper half of the complex plane can be expressed as

$$\bar{s}_i = \epsilon + j(1 + \delta) \tag{22}$$

where

$$\epsilon^2, \delta^2 \ll 1 \tag{23}$$

For small enough gains we also have the small product relationships

$$|\zeta_n\epsilon|, |\zeta_n\delta|, |k'\delta|, k'\epsilon|, |k\delta|, |k\epsilon|, |k\zeta_n|, |k'\zeta_n| \ll 1 \tag{24}$$

and that the root departures from the ith mode pole are small compared to the separation of the ith mode pole from all but the closest of the other modal poles, so that

$$\epsilon^2, \delta^2 \ll |(1 - r_n^2)/2|^2 \quad n \neq i,m \tag{25}$$

where m is the mode whose natural frequency is closest to that of the ith mode.

For small gains, substituting Eq. (22) into Eq. (17), and making use of inequalities Eqs. (23–25), we obtain (neglecting higher-order quantities)

$$[-\delta + j(\zeta_i + \epsilon)]^2 + [-\delta + j(\zeta_i + \epsilon)] \times \left[\left(\frac{k'j + k}{2}\right)(u_ma_m + u_ia_i) - \left(\frac{1 - r_m^2}{2}\right)\right] - \frac{(k'j + k)}{2} u_ia_i \left(\frac{1 - r_m^2}{2}\right) = 0 \tag{26}$$

By solving Eq. (26) for $[-\delta + j(\zeta_i + \epsilon)]$, and then equating real and imaginary parts, we can obtain the roots near the ith and mth modal poles. Equation (26) is useful for estimating the roots when two natural frequencies are close together, or when the first mode natural frequency is close to that of the rigid mode.

In the more common case (which is treated in special detail here) the modal frequencies are well separated so that

$$\epsilon^2, \delta^2, \ll |(1 - r_m^2)/2|^2 \tag{27}$$

and Eq. (26) yields the relative departure of the upper half complex plane ith mode root from its pole as

$$\epsilon = -k' (u_ia_i/2) - \zeta_i \tag{28}$$

$$\delta = k (u_ia_i/2) \tag{29}$$

For k fixed, it is evident from Eq. (28) that the roots always leave the imaginary axis at 0° or 180° as k' is increased.

§ A typical stable root locus plot for K_v is shown in Fig. 7.

(This conclusion assumes that the actuator and sensor have negligible phase shift at the flexural frequencies considered. This is discussed further in Sec. B.) Therefore, for the simple control considered here, for stability of the ith mode without structural damping it is only necessary that

$$\text{sgn} u_i = \text{sgn} a_i \tag{30}$$

If for given locations of the actuator and sensor, Eq. (30) is true for all modes, then the entire system will be stable.

The effective gains k' and k decrease rapidly with mode number [as is evident from Eqs. (20) and (21)]; therefore, for the case where $|u_n a_n|$ does not increase with mode number, Eqs. (28) and (29) will yield a good approximation to the higher modal roots. It should also be observed that for this case the damping of the higher modal roots with control will be determined primarily by structural damping, and therefore the very high-frequency modes will not be troublesome with normal structural damping.

Equations (28) and (29) may also be used to approximate the first flexural modal root, their validity depending on how well the assumptions are satisfied (particularly the separation of the frequency of the first mode from the rigid body mode).

Using Eqs. (13) and (20) we can also express ϵ in terms of the rigid mode damping ratio with control, ζ_{co}, as

$$\epsilon = -(\zeta_{co}/p_i)\,(p_o^2 + K_p)^{1/2} u_i a_i - \zeta_i \tag{31}$$

for the cases for which Eq. (13) yields a satisfactory answer even though flexure is included.

B. Use of Other Linear Controllers

A similar perturbation analysis can be performed for linear controllers other than the pure position and rate feedback control just illustrated. Reference 3 carries out the perturbation analysis for the use of a rate network in place of pure rate. Again, neglecting structural damping, no root locus crosses the imaginary axis, so that the criterion for stability is still that of Eq. (30), with the higher mode roots staying closer to the poles than for the pure rate case.

In general, when additional poles and zeros appear in the characteristic equation in series with those due to position and rate feedback, the angle of departure from the ith mode pole (with k fixed) will simply be that obtained with pure rate feedback alone (determined by the sgn $u_i a_i$), then shifted in angle to account for the phase change at the pole due to the additional poles and zeros. For the cases where the higher mode roots stay relatively close to their poles, the angle of departure is usually all that is required to determine their stability.

C. Real Time Response

An estimate of the real time response can be obtained for small gains by substituting the roots obtained by the expansion method into the system transfer function and taking the inverse Laplace Transform. Thus when the roots obtained from Eqs. (28) and (29) are substituted into Eq. (14), we obtain the real time response of the ith mode to a unit step input, for $k = 0$, as

$$\mu_i(t) \approx \frac{K_v}{p_i}\,|u_i a_i| \left\{ \exp\left[-\left(K_v \frac{u_i a_i}{2} + \zeta_i p_i \right) t \right] \right\} \sin p_i t \tag{32}$$

Observe that when $|u_i a_i|$ does not increase with mode number, the amplitude of the response of the higher modes to a step input diminishes rapidly as the natural frequency of the mode increases. For ζ_i approximately constant with i, the time constant of decay rapidly decreases so that for the higher modes the time constant associated with ζ_i will usually dominate compared to the time constant associated with the control.

The steady-state frequency response of the stable system can be obtained in the standard manner by setting $s = j\omega$ in the system transfer function. When this is done in Eq. (14), it is shown in Ref. 3 that for the flexural modes with frequencies well above the forcing frequency their excitation is small and they can be ignored when $|u_n a_n|$ does not increase with mode number.

D. Physical Interpretation

In deriving the general approach it was observed that, for ϵ and δ small compared to the separation of frequencies, the characteristic roots of the system associated with the ith mode were relatively independent of the other modes. Therefore, referring to Fig. 1, for the purpose of deriving the ith mode roots we can consider the system to be just the ith mode of flexure with the feedback loop around it.

Physically this can be interpreted as follows. If the ith mode is excited, then it will respond at its loop resonant frequency. If ϵ is small compared to the frequency separation, then the ith mode will be relatively undamped and have a high Q (amplification ratio) at this frequency compared to the other modes (δ must also be small compared to the frequency separation to maintain the frequency separation large compared to ϵ). Thus the ith mode passes its loop resonant frequency very readily compared to the other modes, which can be considered to be effectively blocked off.

If another frequency is close to the ith frequency compared to ϵ, δ, or ζ, then it will have a sufficiently high response at the ith mode loop frequency so that it must be considered. In that case we have a quadratic expression determining the ϵ and δ, as in Eq. (16).

For the case where the frequencies are well separated, each mode must be stabilized independently. As there is only one controller, an undesired sign reversal must be avoided in the loop. Therefore for a system with simple rate and position feedback, the sign of u_n must be the same as the sign of a_n.

If, besides rate and position feedback, there are additional leads or lags in series with the gain, the following observations can be made. If these leads or lags have time constants that are small compared to the period of the rigid mode loop, then they have very little effect upon it. However, as we consider the higher modes, it is found that a point may be reached where the control is applied too early or too late so that it tends to aid the deflection rather than retard it, which in turn leads to instability for an otherwise stable mode or, conversely, perhaps leads to stability for an otherwise unstable mode.

E. The $u_n a_n$ Relationships for Attitude Control of a Simple Beamlike Flexible Vehicle

The relationship of u_n and a_n to the positions of the forces and sensors along the mode shape can be illustrated by considering a simple position and rate feedback attitude control system for a flexible rocket, missile, or satellite employing a lateral force F at the aft end for attitude control. (Complicating factors, such as fuel slosh, are neglected so that for the purposes of this discussion the vehicle can be characterized as a simple beam.) For such a simplified vehicle, utilizing Eqs. (2–4), the $u_n a_n$ relationships shown in Fig. 2 apply.

Comparing the first mode in Fig. 2b to the rigid body mode in Fig. 2a, it is found that $u_1 > 0$, but for the sensor location shown the sensor reads a negative angle for a positive q_1, so that $a_1 < 0$. Thus we have a sign reversal as we go around the first mode loop. If the first mode shape were normalized instead so that q_1 is positive upward, as shown in Fig. 2c, then the sensor would read a positive angle for a positive q_1, so that $a_1 > 0$; but observe that then $u_1 < 0$. It is apparent that, as the way we normalize a mode shape is arbitrary, stability depends only upon the sign of the product $u_i a_i$, not upon the signs of the terms themselves.

From Fig. 2d, we observe that the second mode is stable, even though the first mode is unstable. It is readily apparent

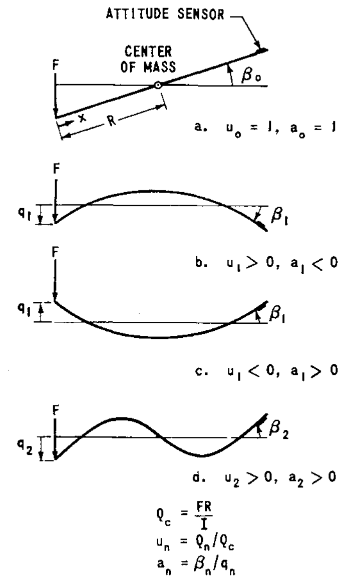

Fig. 2 The u_n and a_n relations for attitude control of a simplified flexible rocket.

that to insure that all the modes are stable (no sign reversal in any modal loop), we need only place the control force and the sensor together at either end of the vehicle, for at the extremities of the vehicle the signs of the slopes and deflections are the same for all modes.

Observe from Fig. 3 that simply putting the control force and sensor together at an arbitrary location does not insure that the sign of $u_n a_n$ will be positive. Thus position A yields $u_1 a_1 > 0$, whereas B yields $u_1 a_1 < 0$. Therefore with a control system employing simple position and rate feedback, the first mode would be unstable for position B, and stable for position A.

V. Applications

The general approach we have presented and the equations which we have derived are applicable to a large variety of flexible vehicles. To illustrate this we will consider in detail the examples presented in Section IV and several additional ones. Though the signs of u_n and a_n can be determined by visual inspection of the modeshapes, it is worthwhile to show how numerical values can be assigned to them and for simple position and rate feedback to present the resulting root locus computer solution associated with Eq. (17).

A. Attitude Control of Simple Beamlike Vehicles

The vehicles illustrated in Figs. 2 and 3 are examples of attitude control of flexible vehicles which can be represented by a beam controlled by applied forces. If we consider the simplified case where the vehicle is assumed to be represented by a uniform free-free beam, then from Refs. 6 or 7, the normalized, nth mode shape is given by

$$w_n(\xi) = \tfrac{1}{2}\{\cosh b_n\xi + \cos b_n\xi - C_n(\sinh b_n\xi + \sin b_n\xi)\} \quad (33)$$

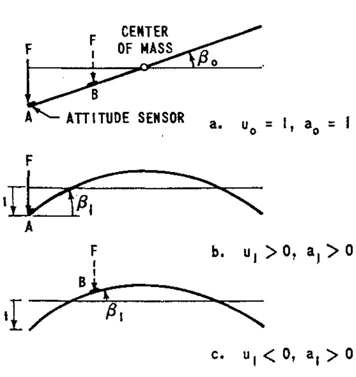

Fig. 3 The u_n and a_n relations for a simplified vehicle attitude system with the control force and sensor at a single location, as a function of that location.

where

$$\xi = x/L = (\text{distance from aft end})/(\text{length of vehicle}) \quad (34)$$

and b_n and C_n are constants associated with the nth mode, and the deflection is positive up as in Fig. 2c.

For such a beam with a control force at station x, employing Eqs. (3, 4, 33, and 34), the nth mode generalized force and mass reduce to

$$F_n = \int_0^L w_n(x)f(x)dx = -F(\xi)w_n(\xi) \quad (35)$$

$$M_n = \int_0^L m(x)w_n^2(x)dx = M\int_0^1 w_n^2(\xi)d\xi = \frac{M}{4} \quad (36)$$

where $M = mL$, the total mass of the vehicle.

The rigid mode forcing function is given by

$$Q_c = F(x)(R - x)/I = F(x)(R - x)/M(R^2/3) = 3F(\xi_f)(1 - 2\xi_f)/MR \quad (37)$$

thus

$$u_n = Q_n/Q_c = (F_n/M_n)/Q_c = -w_n(\xi_f)R/0.75(1 - 2\xi_f) \quad (38)$$

$$a_n = \beta_n/q_n = \partial w_n(x)/\partial x = (1/2R)\,(\partial w_n/\partial\xi)(\xi_s) \quad (39)$$

therefore

$$u_n a_n = -w_n(\xi_f)(\partial w_n/\partial\xi)\,(\xi_s)/[1.5\,(1 - 2\xi_f)] \quad (40)$$

where the subscript f pertains to the force, and the subscript s pertains to the sensor.

Observe that $u_n a_n$ is independent of the size of the vehicle, being just a function of the manner in which the mass and stiffness are distributed (uniform in our case), and the relative force and sensor locations.

Figure 4 is a computer generated root locus, corresponding to Fig. 2, for the case where the force and sensor are at opposite ends of the vehicle and the first mode natural frequency is four times that of the undamped rigid mode frequency with control.

Figures 5 and 6 are the root loci for the force and sensor together at the left end and at $\xi = 0.34$, respectively, corresponding to locations A and B in Fig. 3.

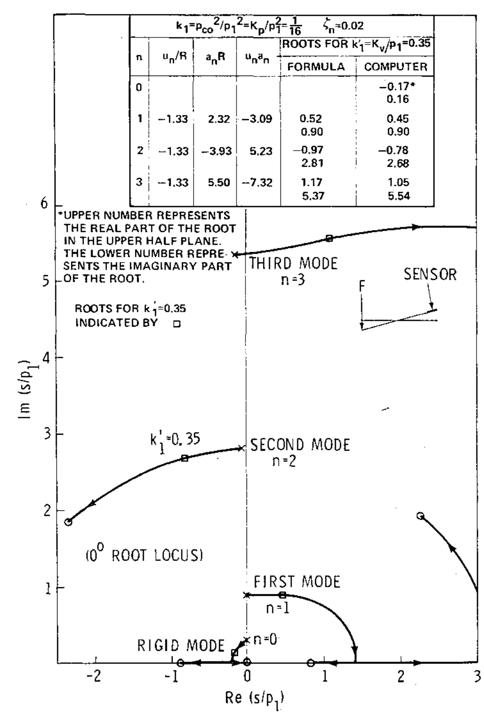

$k_1 = p_{co}^2/p_1^2 = K_p/p_1^2 = \frac{1}{16}$ $\zeta_n = 0.02$

n	u_n/R	a_nR	u_na_n	ROOTS FOR $k_1' = K_v/p_1 = 0.35$ FORMULA	COMPUTER
0					−0.17* 0.16
1	−1.33	2.32	−3.09	0.52 0.90	0.45 0.90
2	−1.33	−3.93	5.23	−0.97 2.81	−0.78 2.68
3	−1.33	5.50	−7.32	1.17 5.37	1.05 5.54

Fig. 4 Root locus of a simplified flexible rocket, force at left, sensor at right.

Numerical results are indicated on the figures using both the simple modal root formulas, Eqs. (28) and (29), and the computer solutions, for a rigid mode damping ratio due to control of approximately 0.7. Observe that satisfactory numerical agreement is shown for Figs. 4 and 6. For the roots corresponding to Fig. 5 it is clear that the assumption of small root departures, Eqs. (23) and (25), is violated, so that the results of applying the formula in this case is only indicative of stability and large root departures.

B. Train Autopilot

If after bringing a train to a desired speed, we wish to relieve the engineer of the task of maintaining this speed, we can use a simple velocity feedback control system, resulting in a system block diagram of the type shown in Fig. 1. (Essentially the same control would be achieved by the engineer if he responds rapidly to the speedometer reading.)

As a first approximation to a flexible train, we can consider it to be a uniform bar, with both ends free, that can undergo longitudinal vibration. For such a bar, the mode shapes of elongation are[7]

$$w_n(x) = \cos n\pi\, x/L \;(n = 1 \text{ to } N) \tag{41}$$

where x is the position along the train going towards the rear and L is the length of the train.

For this case, employing Eqs. (3, 4, 7, and 8), we find that

$$u_n = 2\, w_n(x_f) \tag{42}$$

$$a_n = w_n(x_s) \tag{43}$$

thus

$$u_n a_n = 2\, w_n(x_f) w_n(x_s) = 2\, w_n(\xi_f) w_n(\xi_s) \tag{44}$$

Observe that the system will always be stable if the force and sensor are located together (e.g., in the locomotive) as is common practice. Figure 7 is a root locus for the locomotive at the head or rear of the train, while Fig. 8 is the solution for the locomotive in the middle of the train. The roots for a velocity gain of $K_v = 0.1g/16$ fps are indicated on the figures, assuming that the first mode frequency is 1 rad per sec.

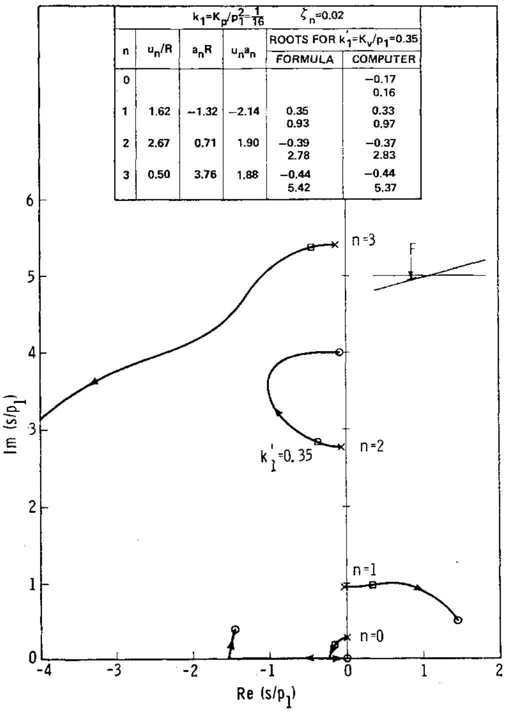

$k_1 = K_p/p_1^2 = \frac{1}{16}$ $\zeta_n = 0.02$

n	u_n/R	a_nR	u_na_n	ROOTS FOR $k_1' = K_v/p_1 = 0.35$ FORMULA	COMPUTER
0					−0.17 0.16
1	1.62	−1.32	−2.14	0.35 0.93	0.33 0.97
2	2.67	0.71	1.90	−0.39 2.78	−0.37 2.83
3	0.50	3.76	1.88	−0.44 5.42	−0.44 5.37

Fig. 6 Root locus for a uniform beam-like vehicle, force and sensor at $x/L = 0.34$.

If the velocity sensor is placed in the caboose and the locomotive is at the head of the train, then from Eq. (44), $u_na_n = 2(-1)^n$ and the odd modes will be unstable.

C. Servo for Positioning a Shaft

If we have a shaft supported by bearings that we desire to position in response to an angular input, we could use the simple position and rate feedback control of Eq. (10). If we consider a uniform shaft, the torsional mode shapes $w_n(x)$ are identical with those for longitudinal vibration.[7] Thus we

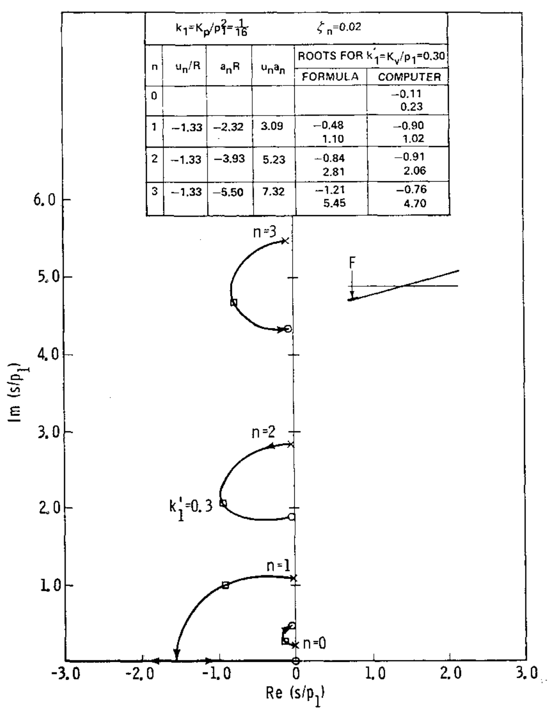

$k_1 = K_p/p_1^2 = \frac{1}{16}$ $\zeta_n = 0.02$

n	u_n/R	a_nR	u_na_n	ROOTS FOR $k_1' = K_v/p_1 = 0.30$ FORMULA	COMPUTER
0					−0.11 0.23
1	−1.33	−2.32	3.09	−0.48 1.10	−0.90 1.02
2	−1.33	−3.93	5.23	−0.84 2.81	−0.91 2.06
3	−1.33	−5.50	7.32	−1.21 5.45	−0.76 4.70

Fig. 5 Root locus of a simplified flexible rocket, force and sensor at left end.

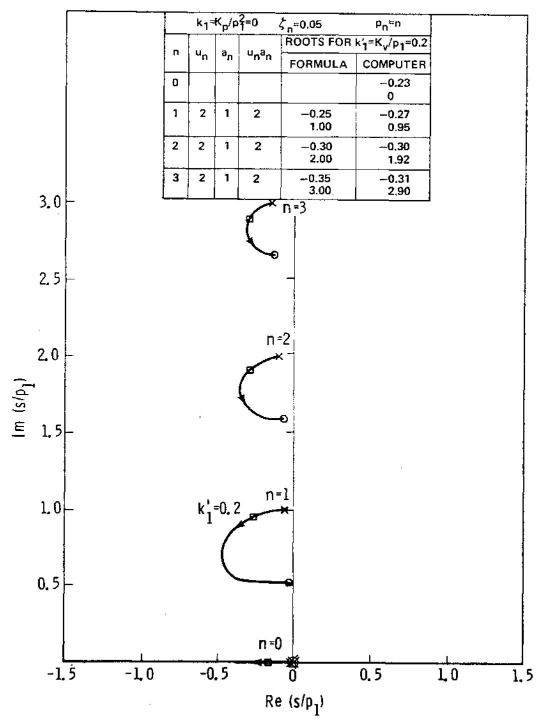

$k_1 = K_p/p_1^2 = 0$ $\zeta_n = 0.05$ $p_n = n$

n	u_n	a_n	u_na_n	ROOTS FOR $k_1' = K_v/p_1 = 0.2$ FORMULA	COMPUTER
0					−0.23 0
1	2	1	2	−0.25 1.00	−0.27 0.95
2	2	1	2	−0.30 2.00	−0.30 1.92
3	2	1	2	−0.35 3.00	−0.31 2.90

Fig. 7 Root locus of a train autopilot, engine and speedometer in front.

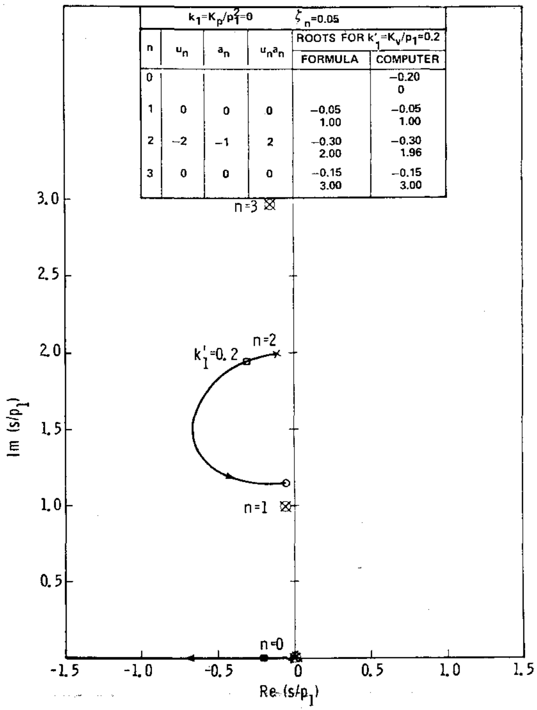

$k_1=K_p/p_1^2=0$				$\zeta_n=0.05$	
n	u_n	a_n	u_na_n	ROOTS FOR $k_1'=K_v/p_1=0.2$	
				FORMULA	COMPUTER
0					−0.20 0
1	0	0	0	−0.05 1.00	−0.05 1.00
2	−2	−1	2	−0.30 2.00	−0.30 1.96
3	0	0	0	−0.15 3.00	−0.15 3.00

Fig. 8 Root locus of a train autopilot, locomotive in middle of train.

obtain the identical u_na_n relations for the shaft as we did for the train, by simply letting the subscript f correspond to the torquer in Eq. (44). As a result, we arrive at the same conclusions for the shaft as we did for the train. Thus if we place the torquer and sensor at opposite ends of the shaft, u_na_n will be negative for n odd and we would have a root locus similar to that of Fig. 4.

VI. Summary and Conclusions

In this paper we have developed relations indicating that the u_n's and a_n's, associated with the actuator and sensor locations, are the important flexural coupling parameters to be considered in the control of a flexible vehicle. For the case of position and rate feedback, we have developed simple approximate formulas for obtaining the system roots, determining stability, and estimating real time response for small gains. We have indicated how the same approach might be used for other linear controllers, such as the use of a lead lag rate network. It is also apparent that the same modal root expansion approach can be used to obtain the roots at larger values of gains and root departures, by retaining higher order terms, as is done in Ref. 3.

From consideration of the general root expansion approach, we can reach some general conclusions for any flexible vehicle employing a feedback control system with uncoupled control axes

1) The stability of the nth mode is dependent on the sign of u_na_n.

2) For vehicles which can be characterized as beams, it is unlikely that all flexible modes can be stabilized without structural damping, unless the rotational sensor and the control force for each axis are placed where the signs of the slope and deflection are the same for all modes, such as the beginnings or ends of the mode shapes.

3) For beamlike vehicles, simply placing the sensor and the control force together at an arbitrary location is insufficient to insure that u_na_n will be either positive or negative or that the system will be stable. However, when u_n varies in the same fashion as a_n along the mode shape, such as when we apply a moment and measure the resulting angle in a torsion or bending problem, then placing the moment and sensor together is sufficient to insure that u_na_n will be positive.

4) For vehicles employing linear feedback control systems: a) The control gains associated with the rigid mode usually have very little effect on the roots of the higher modes, so that the extent of their stability is primarily determined by their own structural damping ratio. b) The uncoupling of the roots of one mode from those of the other modes, for small gains, can be attributed physically to the resonance phenomenon (for small damping) of the nth mode at its own loop frequency, and the relatively low response of the other modes to this frequency due to the separation of modal frequencies.

References

[1] Andrew, G. M. and Johnson, J. M., Jr., "Automatic Control of Aeroelastic Modes," IAS paper 62-86, June 1962, IAS.

[2] Gevarter, W. B., "Analysis of the Stability of a Flexible Space Vehicle During Powered Flight," LMSC 658720, 1964, Lockheed Missiles & Space Co., Sunnyvale, Calif.

[3] Gevarter, W. B., "Attitude Control of a Flexible, Spinning, Toroidal, Manned Space Station," Rept. 250, 1965, Dept. of Aeronautics and Astronautics, Stanford Univ., Stanford, Calif.; also Ph.D. dissertation, Dec. 1965, Stanford Univ.

[4] Biggs, J. M., *Introduction to Structural Dynamics*, McGraw-Hill, New York, 1964, pp. 116–146, 329–332.

[5] Kalman, R. E., "When Is a Linear Control System Optimal," *Transactions of the ASME, Ser. D: Journal of Basic Engineering*, Vol. 86, No. 1, March 1964, pp. 51–60.

[6] Young, D. and Felgar, R. P., Jr., "Tables of Characteristic Functions Representing Normal Modes of Vibration of a Beam," Publication 4913, July 2, 1949, Univ. of Texas.

[7] Volterra, E. and Zachmanoglou, E. C., *Dynamics of Vibration*, Charles E. Merrill Books, Columbus, Ohio, 1965, pp. 296, 297, 303–306, 310–322.